Compact Skyrmions, Merons and Bimerons in Thin Chiral Magnetic Films

Motohiko Ezawa
Department of Applied Physics, University of Tokyo, Hongo 7-3-1, 113-8656, Japan
(Dated: October 21, 2010)

A meron is a controversial topological excitation because it carries just one half of the topological charge unit. It is believed that it is tightly binded to another meron and cannot be observed by isolating it. We present a counter example, investigating the 2-dimensional nonlinear sigma model together with the Dzyaloshinskii-Moriya interaction, where topological excitations are merons, bimerons and skyrmions. They behave as if they were free particles since they are electrically neutral. A prominent feature is that the topological charge density is strictly confined within compact domains. We propose an analytic approach for these compact excitations, and construct a phase diagram. It is comprised of the helix, meron, skyrmion-crystal, skyrmion-gas and ferromagnet phases. It explains quite well the experimental data recently performed in chiral magnets such as MnSi and FeCoSi thin films, as verifies that merons are surely basic topological excitations in the system.

Topological excitations are endlessly fascinating. They are constantly under investigations in all branches of physics. Well known examples are vortices and skyrmions[1]. A fantastic topological object is a meron: It cannot exist by itself since it carries only one half of the topological charge unit. A meron was originally invented as a half-instanton in the context of quark confinement in particle physics[2]. Later it was introduced as a half-skyrmion in order to account for a certain anomalous behavior in bilayer quantum Hall effects[3]. Though the meron is a theoretically useful concept, it remains to be a long-standing problem whether it exists in reality. There is no clear evidence for its existence in spite of experimental endeavors[1].

Magnetic thin films are ideal systems to investigate and test various intriguing ideas on topological excitations. Indeed, a skyrmion crystal[4] as well as a single skyrmion[5] have been observed in chiral magnets such as MnSi and FeCoSi thin films. Furthermore, magnetic domains observed in ferromagnets such as a TbFeCo thin film[6] are shown to be giant skyrmions[7] as large as $\sim 1\mu m$. In this paper we point out that merons are also detectable as almost isolated objects.

The ground state of a chiral magnet is a helical state in the absence of external magnetic field. The spin texture of the helical state has a stripe-domain structure, where the width of a stripe has a fixed value determined by sample parameters. A stripe breaks into pieces as the magnetic field increases. By calculating the topological charge density, we show that the endpoint of a broken stripe has the topological charge $Q_{\text{sky}} = 1/2$. It is natural to identify them as merons. Finite-length stripes are bimerons [Fig.1], among which the shortest ones are skyrmions.

When we talk about skyrmions in the 2-dimensional space, it is implicit to assume a Belavin-Polyakov skyrmion. Its spin texture approaches the ground-state value only polynomially at large distance. On the contrary, a skyrmion must be strictly compact in the chiral magnet since it is embedded within a stripe-domain structure. We propose an analytic scheme to explore compact skyrmions, merons and bimerons. Being electrically neutral excitations, they behave as if they were free particles. Based on this observation we construct a phase diagram of the chiral ferromagnet. It explains quite well the recent experimental data carried out in a FeCoSi thin film[5]. This fact shows that the identification of merons is justified not only theoretically but also experimentally.

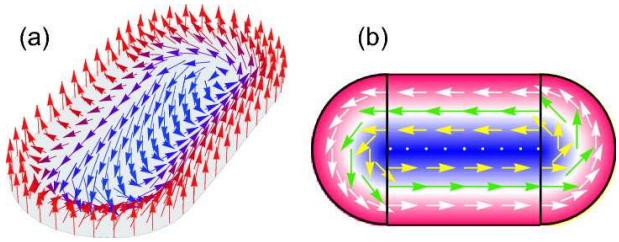

FIG. 1: (Color online) (a) The spin texture of a compact bimeron in a thin chiral magnetic film. (b) A compact bimeron is composed of two half-disk domains and a rectangular stripe domain. Spins are pointed up on the boundary and down deep inside of the bimeron. They are pointed forward and backward in the recutangular part, and twisting circularly in the half-disk part. The topological charge density is nonvanishing only in the half-disk parts, each of which has $Q_{\text{sky}} = 1/2$. The half-disk part is identified as a meron. The spin texture of a compact skyrmion is obtained simply by removing the recutangular part and by patching the two half-disk domains.

Our system is the 2-dimensional plane described by the nonlinear O(3) sigma model H_J with easy axis anisotropy,

$$H_J = \frac{1}{2}\Gamma \int d^2x \left[(\partial_k \boldsymbol{n}) (\partial_k \boldsymbol{n}) - \xi^{-2} (n_z)^2 \right], \qquad (1)$$

and the Dzyaloshinskii-Moriya interaction (DMI),

$$H_{\text{DM}} = D \int d^2x \, \boldsymbol{n}(\boldsymbol{x}) \cdot (\nabla \times \boldsymbol{n}(\boldsymbol{x})) \,, \qquad (2)$$

where $\Gamma = (1/2) z S^2 J$ is the exchange energy (z denotes the number of nearest neighbors, S the spin per atom, J the exchange constant), ξ is the single-ion easy-axis-anisotropy constant, and $\boldsymbol{n} = (n_x, n_y, n_z)$ is a classical spin field of unit length. The DMI term breaks the chiral symmetry explicitly. We introduce the magnetic field h perpendicular to the plane with the Zeeman energy $\Delta_Z = Sg\mu_B\mu_0 h$,

$$H_Z = -(\Delta_Z / a^2) \int d^2x \, n_z(\boldsymbol{x}), \qquad (3)$$

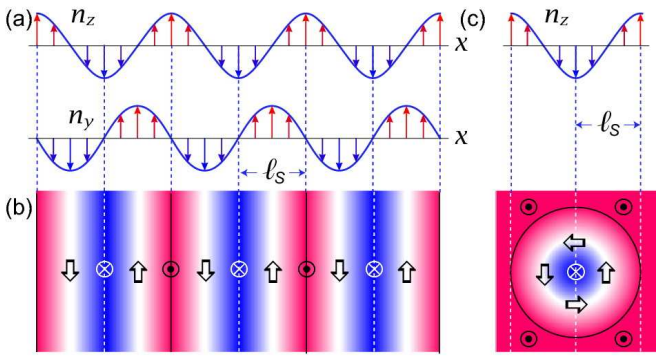

FIG. 2: (Color online) (a) Illustration of the helical state solution $n_i(x)$ described by the Jacobian elliptic function (5). Here we have taken $\kappa = 0.3$. (b) Illustration of the spin structure with an alternating up-down and forward-backward stripe-domains. Spins are strictly pointed up or down on the vertical solid or dotted lines. As one stripe we consider the region sandwiched by two solid lines. (c) Illustration of a compact skyrmion described by the Jacobian elliptic function (10) . It is constructed in such a way that any cross section passing through the center agrees with the cross section of the stripe. The topological charge is strictly confined within the solid circle.

where a is the lattice constant.

We have emphasized previously[7] the importance of the magnetic dipole-dipole interaction (DDI). However, since the DDI constant is very small compared to the DMI constant, we may ignore it in determining the magnetic structure of a chiral magnet. Indeed, the typical size determined by the DMI is of the order of 40nm, where the DDI is negligible.

We start with a study of the system in the absence of external magnetic field. The ferromagnetic spin state $\boldsymbol{n} = (0, 0, \pm 1)$ is a solution of the Hamiltonian $H_{J\text{-DM}} = H_J + H_{\text{DM}}$ with the energy

$$E_{\text{homo}} = -\Gamma/2\xi^2. \tag{4}$$

However, in general, this is not the ground state. It is easy to prove that the Hamiltonian $H_{J\text{-DM}}$ allows one-dimensional periodic solutions, among which the one that minimizes the DMI term (2) is given by

$$\begin{aligned} n_x(x) =& 0, \quad n_y(x) = \text{cn}\left(\frac{x-\ell_S/2}{\kappa\xi}, \kappa^2\right), \\ n_z(x) =& \text{sn}\left(\frac{x-\ell_S/2}{\kappa\xi}, \kappa^2\right), \end{aligned} \tag{5}$$

in terms of the Jacobian elliptic functions [Fig.2(a)], where κ is an integration constant with $0 \le \kappa^2 \le 1$. The periodicity of $\sigma(x)$ is $2\ell_S$ with

$$2\ell_S \equiv 4\kappa\xi K(\kappa^2), \tag{6}$$

where $K(\kappa^2)$ is the complete elliptic integral of the first kind. The periodic state (5) has an alternating up-down and forward-backward spin-stripe structure, as illustrated in Fig.2(b). It may be called the anisotropic helical state. Note that $n_z(-\ell_S) = 1$, $n_z(0) = -1$, $n_z(\ell_S) = 1$. As one stripe we consider the region whose width is $2\ell_S$ with the center line being given by $n_z(x) = -1$.

By substituting (5) into the Hamiltonian $H_{J\text{-DM}}$, the energy of the helical state is analytically calculable,

$$E_{\text{helix}} = L_x L_y \left[\frac{\Gamma}{2\xi^2}\left(\frac{2}{\kappa^2}\frac{E(\kappa^2)}{K(\kappa^2)} - \frac{1}{\kappa^2} + 1\right) - \frac{\pi D}{2\kappa\xi K(\kappa^2)}\right], \tag{7}$$

where L_x and L_y are the sample size in the x and y direction. We determine the parameter κ by minimizing E_{helix} with respect to κ. It is given by solving $2E(\kappa^2) = \kappa\pi D\xi/\Gamma$. Provided $D\xi \gg \Gamma$, it is solved as

$$\kappa = \frac{\Gamma}{D}\frac{1}{\xi} - \frac{1}{4}\left(\frac{\Gamma}{D}\frac{1}{\xi}\right)^3 + \cdots, \tag{8}$$

and the energy of the helical state is

$$E_{\text{helix}} = L_x L_y \left[-\frac{D^2}{2\Gamma} + \frac{\Gamma}{2\xi^2} + \cdots\right]. \tag{9}$$

We compare this with that of the homogeneous state (4). We find that the helical state has a lower energy than that of the homogeneous state if $D\xi > \sqrt{2}\Gamma$. It is interesting that the helical state does not realize in the sample when the anisotropy is too large.

We switch on the external magnetic field. The Zeeman effect enforces the increase of the up-spin region. However, it is impossible to increase only the width of the up-spin part of the stripe, which is fixed to be ℓ_S. The simple way is to split a stripe into two stripes, since it increases up-spin region [Fig.3(a)]. Let us cut one stripe at $y = 0$ and then put a cap so that the spin field on the cross section smoothly approaches the up-spin value at the boundary in order to optimize the energy [Fig.1(b)]. The spin texture of the cap must be given by

$$\begin{aligned} n_x(r,\theta) &= -\text{cn}\left(\frac{r-\ell_S/2}{\kappa\xi}, \kappa^2\right)\sin\theta, \\ n_y(r,\theta) &= \text{cn}\left(\frac{r-\ell_S/2}{\kappa\xi}, \kappa^2\right)\cos\theta, \\ n_z(r,\theta) &= \text{sn}\left(\frac{r-\ell_S/2}{\kappa\xi}, \kappa^2\right), \end{aligned} \tag{10}$$

for the half-disk region ($r \le \ell_S, 0 \le \theta \le \pi$) in the cylindrical coordinate, since it agrees with (5) at $y = 0$, where $\cos\theta = 1$.

A stripe may be broken into three stripes with one finite-length stripe [Fig.3(a)]. The spin structure of a finite-length stripe is illustrated in Fig.1. The shortest stripe is a cylindrical symmetric domain [Figs.3(a) and 2(c)], whose spin texture is described by (10) for the disk region ($r \le \ell_S, 0 \le \theta \le 2\pi$).

The use of a continuum approximation and of classical fields to represent the spins is justified as far as we analyze phenomena whose characteristic wavelength is much larger than the lattice constant. In this regime there exists the topologically conserved charge, that is the Pontryagin number,

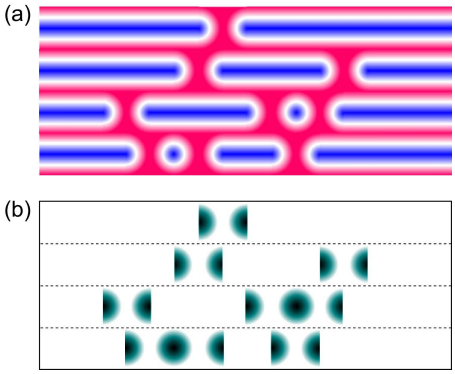

FIG. 3: (Color online) (a) Illustration of compact skyrmions, merons and bimerons embedded in the stripe-domain structure. (b) Illustration of the topological charge density confined within compact domains. Dotted lines show the boundaries of stripes.

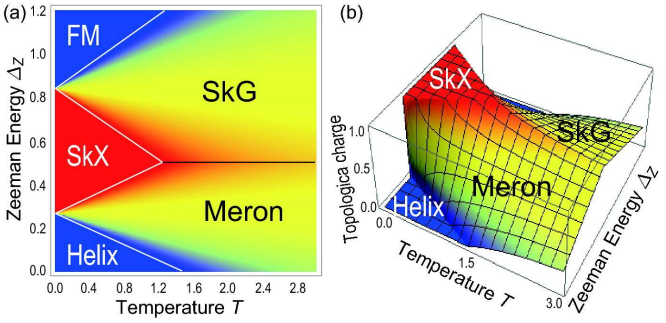

FIG. 4: (Color online) (a) Phase diagram. The horizontal axis is the temperature T in unit of $D^2/k_{\rm B}\Gamma$, while the vertical axis is the Zeeman energy Δ_Z in unit of D^2/Γ. (b) Average topological charge density in various phases.

$Q_{\rm sky} = \int d^2x\, \rho_{\rm sky}(\boldsymbol{x})$, with the topological charge density

$$\rho_{\rm sky}(\boldsymbol{x}) = -\frac{1}{8\pi}\sum_{ij}\varepsilon_{ij}\boldsymbol{n}(\boldsymbol{x})\cdot\left(\partial_i\boldsymbol{n}(\boldsymbol{x})\times\partial_j\boldsymbol{n}(\boldsymbol{x})\right), \quad (11)$$

where i, j run over x, y with ε_{ij} being the completely antisymmetric tensor. We are able to determine the topological charge density for various spin textures.

First, it is trivial to see that the stripe configuration (5) has no topological density. Then, calculating it for the half-disk configuration (10) with $0 \le \theta \le \pi$, we find that $Q_{\rm sky} = 1/2$. Similarly we find $Q_{\rm sky} = 1$ for the cylindrical symmetric configuration (10) with $0 \le \theta \le 2\pi$. Clearly we can identify them as a meron and a skyrmion, respectively. A prominent feature is that the topological charge is strictly confined within a compact domain. Hence we may call them a compact skyrmion and so on. In general, there appear a variety of topological excitations [Fig.3(a)]. We have illustrated the corresponding topological charge density in Fig.3(b). Let us refer to this regime of topological excitations as the meron phase, since the basic excitation is a meron that appears at the endpoint of a stripe.

We now estimate the energy of a topological configuration. The Jacobian elliptic functions are well approximated by the sinusoidal functions when κ is not close to 1, say, $\kappa \lesssim 0.5$. Namely, we may approximated (5) by $n_x(x) = 0$, $n_y(x) = \sin(kx)$ and $n_z(x) = -\cos(kx)$, where $k = 1/\kappa\xi$. This is the well-known expression for the helical ground state in the isotropic system, which is the limit $\xi \to \infty$ with k being fixed. The spin texture of the cap (10) is approximated by

$$n_x(r,\theta) = -\sin(kr)\sin\theta, \quad n_y(r,\theta) = \sin(kr)\cos\theta,$$
$$n_z(r,\theta) = -\cos(kr), \quad (12)$$

for $r \le \pi/2k$. We consider the isotropic system for simplicity.

With the use of the meron configuration (12), by integrating the total Hamiltonian $H = H_J + H_{\rm DM} + H_Z$, it is straightforward to calculate the energy gain when a stripe is broken into two stripes,

$$\Delta E_{\rm merons} = \ell_S^2\left[\left(\frac{4}{\sqrt{3}} - \frac{\pi}{2}\right)\frac{D^2}{\Gamma} - \left(\frac{4}{\pi} + \frac{8}{\sqrt{3}} - \pi\right)\Delta_Z\right]. \quad (13)$$

We may call it the creation energy of a meron pair. The energy gain when a skyrmion emerges in a stripe is just twice of $\Delta E_{\rm merons}$. It follows from (13) that $\Delta E_{\rm merons} < 0$ if $\Delta_Z > \Delta_Z^{\text{Helix-SkX}}$ with

$$\Delta_Z^{\text{Helix-SkX}} = 0.27 D^2/\Gamma. \quad (14)$$

Since the energy gain is negative, all stripes are spontaneously broken into a maximum number of skyrmions for $\Delta_Z > \Delta_Z^{\text{Helix-SkX}}$, which would lead to the formation of a skyrmion crystal (SkX). Namely, $\Delta_Z^{\text{Helix-SkX}}$ is the phase-transition point between the helix and SkX phases. It is concluded that there exists no meron phase at zero temperature.

The SkX has been discussed in literature[8, 9], though Belavin-Polyakov skyrmions are assumed on all lattice points with a certain cutoff. Note that a skyrmion with a cutoff does not have the correct topological charge. We can follow their arguments to study the SkX with the use of compact skyrmions without any problem.

On the other hand, the ferromagnet (FM) phase appears in sufficiently strong external magnetic field, which has only the Zeeman energy, $E_{\rm FM} = -\left(L_x L_y/a^2\right)\Delta_Z$. By comparing this with (13), it follows that the critical Zeeman energy is

$$\Delta_Z^{\text{SkX-FM}} = 0.84 D^2/\Gamma, \quad (15)$$

so that the FM phase appears for $\Delta_Z > \Delta_Z^{\text{SkX-FM}}$.

We proceed to construct the phase diagram in the plane of temperature and magnetic field. We have it already at zero temperature, where there exists only the helix, SkX and FM phases. The meron phase appears at finite temperature, since its entropy is much larger than that of the helix or SkX phase.

In determining the boundary between the helix and meron phases, the basic excitation is a pair of merons in the helix phase [Fig.3(b)]. It appears when a stripe is broken into two pieces with the excitation energy $\Delta E_{\rm merons}$ being given

by (13). Let N be the maximum number of the topological charges (the maximum number of compact skyrmions) that the system can accommodate. When the topological charge of the system is n, the entropy is given by $S = \ln N!/n!\,(N-n)!$. Then, the free energy at temperature T is given by $F = E_{\rm helix} + n\Delta E_{\rm merons} - TS$. Letting $N \to \infty$, we obtain the formula for the free energy density,

$$f = \varepsilon_{\rm helix} + q\Delta E_{\rm merons} + \frac{k_{\rm B}T}{2}\left(q - \frac{1}{2}\right)^2, \qquad (16)$$

where $f = F/N$, $\varepsilon_{\rm helix} = E_{\rm helix}/N$, and $q = n/N$ is the average topological charge density ($0 \le q \le 1$). It is easy to minimize the free energy density f with respect to q. Since f is quadratic in q, it yields two lines starting from the helix-SkX phase-transition point at $T = 0$. They determines the boundary between the helix-meron phases and the boundary between the meron-SkX phases, as illustrated in Fig.4.

The SkX melts into a skyrmion gas (SkG) at higher temperature. We can make a similar argument to derive the boundary between the SkX and SkG phases, where the basic object is a skyrmion in the SkX phase with the excitation energy being

$$\Delta E_{\rm sky} = -\ell_S\left(\frac{\pi D^2}{2\Gamma} + \left(\frac{4}{\pi} - \pi\right)\Delta_Z\right). \qquad (17)$$

We reach at the same formula as (16) with the replacement of $\varepsilon_{\rm helix}$ by $\varepsilon_{\rm SkX}$, and $\Delta E_{\rm merons}$ by $\Delta E_{\rm sky}$. In this way we obtain the boundary between the SkX-SkG phases and the boundary between the SkG-FM phases, as illustrated in Fig.4. Finally, the boundary between the meron and SkG phases is given by $\Delta_Z^{\text{meron-SkG}} = D^2/2\Gamma$ for $T > 4D^2/\pi k_{\rm B}\Gamma$ by comparing their free energies.

The phase diagram thus constructed is characterized by the topological charge density q as follows:

$$q = \begin{cases} 0 & \text{for } \Delta E_i > \frac{1}{2}k_{\rm B}T \quad \text{(Helix, FM)} \\ \frac{1}{2} - \frac{\Delta E_i}{T} & \text{for } |\Delta E_i| < \frac{1}{2}k_{\rm B}T \quad \text{(Meron, SkG)} \\ 1 & \text{for } -\Delta E_i > \frac{1}{2}k_{\rm B}T \quad \text{(SkX)} \end{cases}, \qquad (18)$$

where ΔE_i stands for $\Delta E_{\rm merons}$ or $\Delta E_{\rm sky}$. This phase diagram [Fig.4] captures the essential feature of those obtained experimentally and by a Monte Carlo simulation[5], although they have made no distinction between the meron and SkG phases. We note that the topological charge density q is observable by measuring the Hall conductance σ_{xy} of the topological current[10, 11], $\sigma_{xy} \propto q$.

We remark that all topological excitations have topological charges of the same sign in magnetic thin films. Thus, apparently, a stripe with $Q_{\rm sky} = 0$ breaks into a number of bimerons each of which carries $Q_{\rm sky} = 1$. One may wonder how the topological conservation holds in these systems. We have pointed out previously[7] that a single skyrmion can be created in a thin ferromagnet film by destroying the magnetic order within a tiny spot with the use of photoirradiation. Indeed, the topological charge is well defined only when we can describe the spin system by continuous classical fields. It means that we can break the topological conservation by controlling the system at the lattice-constant scale or at sufficiently high temperature. Thus, in order to create topological excitations, it is necessary to cool the sample from high temperature. Once they are created, their stability is guaranteed topologically. This would be the basic reason why a rich variety of stable spin textures have been observed[5].

We have proposed a new concept of compact topological excitations together with their analytic expressions, based on which we have explored thin chiral magnetic films. Having identified merons as endpoints of stripes, we have pointed out that they have already been observed almost as isolated objects experimentally. The reason why merons can be observed is that they bear no electric charge in magnetic films. Hence, the length of a stripe, which is nothing but a bimeron, is a zero-energy mode. This allows a meron to behave effectively as an isolated topological object though it carries only one half of the topological charge unit. It is worthwhile to search for such merons in other branches of physics.

I am deeply indebted to Y. Tokura, Y. Onose, X.Z. Yu and A. Rosch for illuminating discussions and for informing me as to experimental details. I am very much grateful to N. Nagaosa and J.H. Han for fruitful discussions on the subject. This work was supported in part by Grants-in-Aid for Scientific Research from the Ministry of Education, Science, Sports and Culture No. 22740196 and 21244053.

[1] G.E. Brown and M. Rho (eds.), "The Multifaced Skyrmions", World Scientific, Singapore (2010).
[2] C.G. Callan, R. Dashen and D. Gross, Phys. Rev. D **17**, 2717 (1978).
[3] K. Moon, H. Mori, K. Yang, S.M. Girvin, A.H. MacDonald, L. Zheng, D. Yoshioka and S-C. Zhang, Phys. Rev. B **51** 5138 (1995).
[4] Mohlbauer et al., Science 323, 915 (2009); Munzer et al., Phys. Rev. B 81, 041203 (2010).
[5] X. Z. Yu, Y. Onose, N. Kanazawa, J. H. Park, J. H. Han, Y. Matsui, N. Nagaosa and Y. Tokura, Nature, **465**, 901 (2010).
[6] T. Ogasawara, N. Iwata, Y. Murakami, H. Okamoto and Y. Tokura, Appl. Phys. Lett. **94**, 162507 (2009).
[7] M. Ezawa, cond-mat/arXiv:1007.4048 (to be published in Phys. Rev. Lett.)
[8] A. N. Bogdanov and D. A. Yablonskii, Sov. Phys. JETP 68, 101 (1989). A. Bogdanov and A. Hubert, J. Magn. Magn. Mater. 138, 255 (1994).
[9] J. H. Han, J. Zang, Z. Yang, J.-H. Park and N. Nagaosa, Phys. Rev. B 82, 094429 (2010).
[10] J. Ye *et al*., Phys. Rev. Lett. **83**, 3737 (1999): S.D. Yi, S. Onoda, N. Nagaosa, J.H. Han, Phys. Rev. B 80, 054416 (2009).
[11] M. Lee, W. Kang, Y. Onose, Y. Tokura, and N. P. Ong, Phys. Rev. Lett. **102**, 186601 (2009): A. Neubauer, C. Pfleiderer, B. Binz, A. Rosch, R. Ritz, P.G. Niklowitz, and P. Boni, Phys. Rev. Lett. **102**, 186602 (2009).